

# CHAOS AND UNPREDICTABILITY IN EVOLUTION

Michael Doebeli<sup>1,2,3,\*</sup> and Iaroslav Ispolatov<sup>4,\*</sup>

<sup>1</sup>Department of Zoology, University of British Columbia, 6270 University Boulevard, Vancouver, B.C. V6T 1Z4, Canada

<sup>2</sup>Department of Mathematics, University of British Columbia, 6270 University Boulevard, Vancouver, B.C. V6T 1Z4, Canada

<sup>3</sup>E-mail: doebeli@zoology.ubc.ca

<sup>4</sup>Departamento de Física, Universidad de Santiago de Chile, Casilla 302, Correo 2, Santiago, Chile

Received September 18, 2013

Accepted December 3, 2013

The possibility of complicated dynamic behavior driven by nonlinear feedbacks in dynamical systems has revolutionized science in the latter part of the last century. Yet despite examples of complicated frequency dynamics, the possibility of long-term evolutionary chaos is rarely considered. The concept of “survival of the fittest” is central to much evolutionary thinking and embodies a perspective of evolution as a directional optimization process exhibiting simple, predictable dynamics. This perspective is adequate for simple scenarios, when frequency-independent selection acts on scalar phenotypes. However, in most organisms many phenotypic properties combine in complicated ways to determine ecological interactions, and hence frequency-dependent selection. Therefore, it is natural to consider models for evolutionary dynamics generated by frequency-dependent selection acting simultaneously on many different phenotypes. Here we show that complicated, chaotic dynamics of long-term evolutionary trajectories in phenotype space is very common in a large class of such models when the dimension of phenotype space is large, and when there are selective interactions between the phenotypic components. Our results suggest that the perspective of evolution as a process with simple, predictable dynamics covers only a small fragment of long-term evolution.

**KEY WORDS:** Adaptive dynamics, chaos, complex dynamics, high-dimensional phenotype space, logistic competition models.

Evolution generally takes place in complex ecosystems and is affected by many different processes that generate nonlinear dependencies. According to general dynamical systems theory, which has shown that even simple dynamical system can exhibit complicated dynamics (Li and Yorke 1975; May 1976; Bak et al. 1987; Gleick 1988), one would therefore expect that evolutionary dynamics tend to be complicated. However, this is contrary to traditional evolutionary thinking, which is based on metaphors of static fitness landscapes (Wright 1932; Gavrillets 2004; Svensson and Calsbeek 2012), in which evolution is an optimization process. Accordingly, evolution is often envisioned as a dynamical system that converges to an equilibrium in phenotype space, representing the optimally adapted type. It is of course generally acknowledged that over large time scales, evolution is a nonstationary process, but this is usually attributed to long-term

changes in the external environment causing shifts in evolutionary optima.

Static fitness landscapes describe frequency-independent selection whose strength and direction is not affected by the current phenotypic composition of an evolving population. However, it is widely recognized that ecological interactions, such as competition and predation, often lead to frequency-dependent selection, in which the current phenotypic composition of a population determines whether a particular phenotype is advantageous or not (Heino et al. 1998; Schluter 2000; Doebeli 2011). For example, whether it is advantageous to have a preference for a particular type of food depends on the preferences of the other individuals in the population. Frequency dependence generates an evolutionary feedback loop, because selection pressures, which cause evolutionary change, change themselves as a population's phenotype distribution evolves. It is well known that this feedback can produce complicated dynamics in models in which the dynamic variables are the frequencies of a fixed and finite set of different

\*These authors contributed equally to this work.



types in a given population (Altenberg 1991; Nowak and Sigmund 1993; Gavrillets and Hastings 1995; Schneider 2008; Priklopil 2012). However, such models are essentially ecological models, in which chaotic dynamics is the result of coexistence of different types due to frequency-dependent selection. They are ecological models because they describe the dynamics of the (relative) abundance of different types on short, ecological time scales. In particular, the phenotypes or genotypes present in the population never go beyond the finite set initially provided by the model. Perhaps, this essentially ecological nature of these models helps explain why, even though such models have been shown to exhibit complicated dynamics, the possibility of evolutionary chaos does not really play a role in mainstream evolutionary thinking.

It is important to distinguish models for short-term frequency dynamics from evolutionary models in which the dynamic variables are the (mean) phenotypes themselves, and which track the trajectories of such phenotypes in continuous phenotype spaces, under continual input of new mutations, and over long evolutionary time scales. The phase space for this type of model is the space of all possible phenotypes (rather than the space of frequencies of different types). Adaptive dynamics (Dieckmann and Law 1996; Geritz et al. 1998) provides a useful framework for generating models of long-term evolutionary dynamics of phenotypes. Intuitively, adaptive dynamics unfolds as a series of phenotypic substitutions that give rise to evolutionary trajectories in phenotype space. Frequency dependence plays an important role in adaptive dynamics, but most often, this feedback mechanism has been studied in relatively simple scenarios, in which frequency dependence is still generally expected to generate long-term equilibrium dynamics. But even in simple phenotype spaces, frequency dependence can lead to interesting evolutionary phenomena, such as adaptive diversification (Geritz et al. 1998; Doebeli and Dieckmann 2000; Doebeli 2011). In more complicated phenotype spaces containing scalar phenotypes of each of a number of coevolving populations, frequency dependence can generate complicated evolutionary dynamics. For example, coevolution of scalar traits in predator and prey populations can lead to arms races in the form of cyclic dynamics in phenotype space (Dieckmann et al. 1995; Dieckmann and Law 1996; Dercole et al. 2006), and coevolution of scalar traits in a three-species food chain can generate chaotic dynamics in phenotype space (Dercole and Rinaldi 2008). In all these examples, the dynamic variables undergoing evolution are the (mean) traits in the various interacting species, and the trajectories of these traits in combined phenotype space comprising the scalar traits of all interacting species can exhibit complicated dynamics.

Long-term evolutionary dynamics of continuous phenotypes is ultimately driven by birth and death rates of individual organisms. In general, these birth and death rates are determined in a complicated way by many different phenotypic properties, which

could be as diverse as the molecular efficiency of photosynthesis and the height of trees. Therefore, even for single species it is natural to study evolutionary dynamics in high-dimensional phenotype spaces. For frequency-independent selection, evolution is still an optimization process in such spaces, although genetic correlations between phenotypic components may warp the fitness landscape and alter the convergence dynamics to the local optima (Lande 1979). Yet, apart from a few examples (Doebeli and Ispolatov 2010; Gilman et al. 2012), little is known about the expected complexity of the long-term evolutionary dynamics of high-dimensional phenotypes when selection is frequency-dependent. Here, we ask whether frequency dependence due to competition in high-dimensional phenotype spaces of single species yields evolutionary dynamics that are fundamentally different from the equilibrium dynamics resulting from evolution in simple phenotype spaces.

## Model and Results

We use adaptive dynamics theory (Dieckmann and Law 1996; Geritz et al. 1998; Leimar 2009) to study the long-term evolutionary dynamics in a large class of multidimensional single-species competition models. The starting point is the widely used logistic model (Doebeli 2011)

$$\frac{\partial N(x, t)}{\partial t} = rN(x, t) \left( 1 - \frac{\int \alpha(x, y)N(y, t)dy}{K(x)} \right). \quad (1)$$

Here  $N(x, t)$  is the density of individuals of phenotype  $x$  at time  $t$ , and  $K(x)$  is the carrying capacity of a monomorphic population consisting entirely of  $x$ -individuals. The competitive impact between individuals of phenotypes  $x$  and  $y$  is given by the competition kernel  $\alpha(x, y)$ , so that an  $x$ -individual experiences an effective density  $\int \alpha(x, y)N(y, t)dy$ . This model has been used extensively to study the evolutionary dynamics of scalar traits  $x \in \mathbb{R}$  (Doebeli 2011). Here, we assume more generally that  $x \in \mathbb{R}^d$  is a  $d$ -dimensional vector describing  $d \geq 1$  scalar phenotypic properties. We also assume that  $\alpha(x, x) = 1$  for all  $x$ , and that the intrinsic growth rate  $r$  is independent of the phenotype  $x$  and is equal to 1 (in the evolutionary dynamics derived below, the only effect of the parameter  $r$  is to scale time; in particular, the value of  $r$  is irrelevant for the type of attractor of the evolutionary dynamics). To derive the adaptive dynamics of the multidimensional trait  $x$ , we consider a resident population that is monomorphic for trait  $x$ , for which the ecological model (1) has a unique, globally stable equilibrium density  $K(x)$ , regardless of the dimension  $d$  of  $x$ . Assuming that the resident is at its ecological equilibrium  $K(x)$ , the invasion fitness  $f(x, y)$  of a rare mutant  $y$  is its per capita growth rate in the resident population  $x$ ,

$$f(x, y) = 1 - \frac{\alpha(y, x)K(x)}{K(y)}. \quad (2)$$

The selection gradient  $s(x) = (s_1(x), \dots, s_d(x))$  is derived from the invasion fitness as

$$s_i(x) = \left. \frac{\partial f(x, y)}{\partial y_i} \right|_{y=x} = - \left. \frac{\partial \alpha(y, x)}{\partial y_i} \right|_{y=x} + \frac{\partial K(x)}{\partial x_i} \frac{1}{K(x)}. \quad (3)$$

Finally, the adaptive dynamics of the trait  $x$  is

$$\frac{dx}{dt} = M(x) \cdot s(x), \quad (4)$$

where  $M(x)$  is a  $d \times d$  matrix describing the mutational process in the  $d$  phenotypic components (Leimar 2009; Doebeli 2011) (and where  $dx/dt$  and  $s(x)$  are column vectors). In general, the entries of  $M(x)$  depend on the current population size, and hence implicitly on  $x$ , but for simplicity we assume here that  $M(x)$  is the identity matrix, which is a conservative assumption as far as the complexity of the adaptive dynamics (4) is concerned. This assumption can be justified by noting that including nontrivial  $M$ -matrices would lead to evolutionary dynamics that, up to second order, would have exactly the same general form as the evolutionary dynamics that we will derive below.

Complicated dynamics in the form of oscillations can already occur if the selection gradient  $s(x)$  in (4) is linear. For example, if coefficients for a real  $d \times d$  matrix are chosen randomly from a Gaussian distribution, the probability that at least one eigenvalue has a nonzero imaginary part is  $1 - 2^{-d(d-1)/4}$ , and hence rapidly approaches 1 as the dimension  $d$  is increased (Edelman 1997). This illustrates that the likelihood that a randomly chosen linear system of the form (4) has an oscillatory component increases rapidly with  $d$ . To study nonlinear systems, we assume that the complexity of the interactions between phenotypic components in determining ecological properties is contained in the competition kernel  $\alpha(x, y) : \mathbb{R}^d \times \mathbb{R}^d \rightarrow \mathbb{R}$ , which is in general a complicated, nonlinear function that reflects selective interactions between the different phenotypic components. (Mathematically, selective interactions are present when  $\partial^2 s_i / \partial x_j \partial x_k \neq 0$  for some  $i, j, k$ .)

To keep things as simple as possible while considering nonlinear feedback mechanisms, we consider the Taylor expansion of the competition kernel up to second order. Retaining higher-order terms would only serve to make the feedback mechanisms more complicated, and for our purposes considering only linear and quadratic terms is thus conservative. Up to quadratic terms, and absorbing constant terms into a change of coordinates, we get

$$\left. \frac{\partial \alpha(y, x)}{\partial y_i} \right|_{y=x} \approx - \sum_{j=1}^d b_{ij} x_j - \sum_{j,k=1}^d a_{ijk} x_j x_k. \quad (5)$$

For the carrying capacity, we assume a simple symmetric form:  $K(x) = \exp(-\sum_i x_i^4/4)$ . Because the gradient of the competition kernel is quadratic, this choice of the carrying capacity ensures that the trajectories of the adaptive dynamics (4) are confined to a finite region of phenotype space (because the terms  $\partial K(x)/\partial x_i \cdot$

$1/K(x)$  in (4) are equal to  $-x_i^3$ , and hence dominate for large  $x_i$ ). We note that with our choice for  $K(x)$ , the component of the selection gradient (3) that is due to the carrying capacity does not exhibit selective interactions between different phenotypic components. As a consequence, with trivial competition kernels, the adaptive dynamics (4) would simply be a hill-climbing process toward the unique maximum of the carrying capacity at 0. Thus, any evolutionary complexity originates in the competition kernel (5).

With the above assumptions, the adaptive dynamics (4), describing the evolution of the multidimensional phenotype  $x$ , becomes

$$\frac{dx_i}{dt} = \sum_{j=1}^d b_{ij} x_j + \sum_{j,k=1}^d a_{ijk} x_j x_k - x_i^3, \quad i = 1, \dots, d. \quad (6)$$

The parameters  $b_{ij}$  and  $a_{ijk}$  reflect the selective interactions among the  $d$  phenotypic components. If  $b_{ij} = 0$  for  $i \neq j$  and  $a_{ijk} = 0$  for  $i \neq j, k$ , there are no selective interactions between the phenotypic components, and in that case, the adaptive dynamics (6) always converges to an equilibrium in phenotype space. Thus, if system (6) exhibits complicated dynamics, it must be due to selective interactions. To address the question of the ubiquity of complex evolutionary dynamics, we chose, for a given dimension  $d$  of phenotype space, many different sets of parameters  $b_{ij}$  and  $a_{ijk}$ , reflecting a wide range of possible selective interaction structures for the phenotypic components. Specifically, parameters were drawn randomly from a Gaussian distribution with mean zero and variance 1, and for each choice of parameters evolutionary trajectories were obtained by integrating the adaptive dynamics (6) numerically starting from a random initial condition. We show in section B of the Supporting Information (Fig. S3) that the results are qualitatively the same for any distribution of the coefficients  $b_{ij}$  and  $a_{ijk}$  with a finite variance, and that the results remain true if the coefficients are rescaled such the total strength of selective interactions is independent of the dimension  $d$  of phenotype space.

Chaos is typically defined using the notion of ‘‘Lyapunov exponents,’’ which measure the divergence between two trajectories with similar (but not identical) initial conditions (Devaney 1986). If all Lyapunov exponents of a dynamical system are negative, then the system has a stable equilibrium point. If some Lyapunov exponents are negative and some are (close to) 0, the system exhibits stable limit cycles or quasi-periodic behaviour, in which the system essentially cycles but may not return exactly to previous positions. Finally, chaos is defined by the presence of Lyapunov exponents that are substantially above 0, which indicate that trajectories starting from similar initial conditions diverge over time, essentially leading to unpredictability (the ‘‘butterfly effect’’). To determine the types of dynamics in dynamical

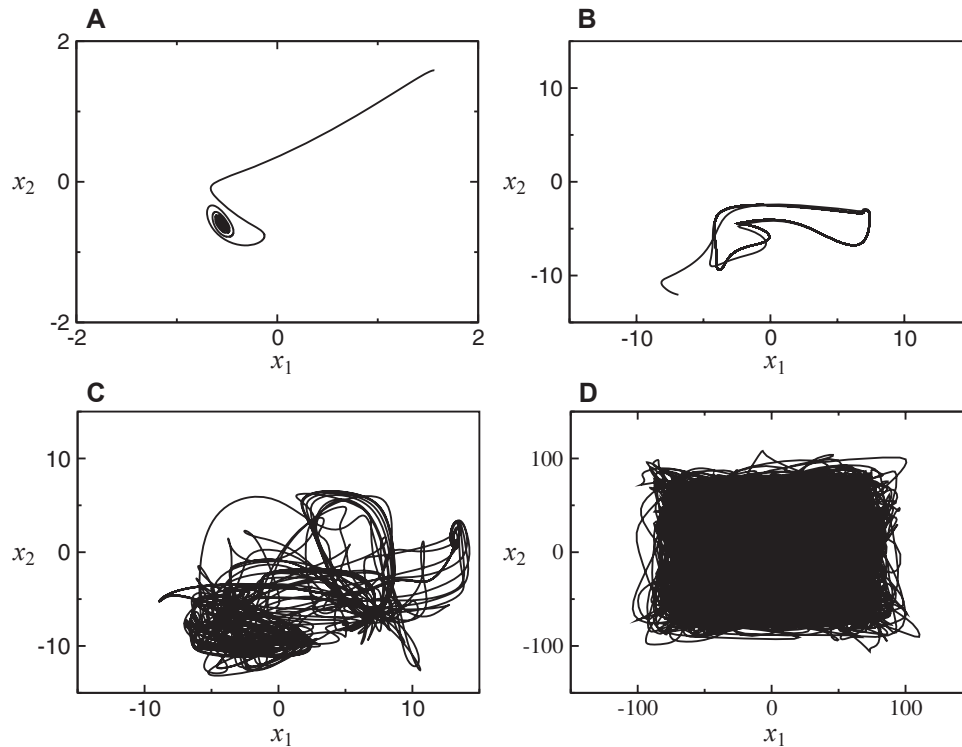


**Figure 1.** A) Example of equilibrium dynamics for  $d = 5$ ; largest Lyapunov exponent  $\lambda = -0.12$ . B) Example of quasi-periodic dynamics for  $d = 15$ ; largest Lyapunov exponent  $\lambda = 0.008$ . C) Example of chaotic dynamics on a non-ergodic (“strange”) attractor for  $d = 15$ ; largest Lyapunov exponent  $\lambda = 1.35$ . D) Example of ergodic chaotic dynamics for  $d = 100$ ; largest Lyapunov exponent  $\lambda = 1850$ . The trajectory essentially fills the phenotype space on a scale of  $(-d, d)$  in each phenotypic dimension. Here and below the integration of (6) was performed from  $t = 0$  to  $t = 400/d^2$  using a 4th-order Runge-Kutta method with time step  $dt = 0.1/d^2$ . The coefficients  $a_{ij}$  and  $b_{ijk}$  were randomly drawn from a Gaussian distribution with zero mean and unit variance, and the initial conditions were randomly drawn from a Gaussian distribution with mean 0 and variance  $d^2$ . The panels show projections of the evolutionary trajectories onto a randomly chosen 2-dimensional subspace of the phenotype space.

systems of the form (6), we measured, for each trajectory, the time average of the largest Lyapunov exponent  $\lambda$  (Devaney 1986) (see Appendix). Based on the largest Lyapunov exponents, we then classified the evolutionary trajectories into three groups: fixed points ( $\lambda < -0.1$ ), periodic or quasi-periodic attractors ( $|\lambda| < 0.1$ ), and chaotic attractors ( $\lambda > 0.1$ ). Examples are shown in Figure 1.

Our main result is that the probability of chaos increases with the dimensionality  $d$  of the evolving system, approaching 1 for  $d \sim 75$  (Fig. 2). Moreover, our simulations indicate that already for  $d \gtrsim 15$ , the majority of chaotic trajectories essentially fill out the available phenotype space over evolutionary time (Fig. 1D), that is, they become “ergodic” (Devaney 1986). An ergodic trajectory essentially visits all areas of phenotype space, and hence fills out the available phenotype space over evolutionary time. The size of the filled phenotype space scales approximately as  $|x_i| < d$  for each phenotypic dimension  $i$  (Supporting Information, section A, Figs. S1 and S2), and the density of trajectories exhibits a universal probability distribution (Fig. 3). It is important to note that because these ergodic trajectories fill out large areas of phenotype

space, they are very different from noisy equilibrium points. Finally, we observe that the largest Lyapunov exponent converges to the universal asymptotic  $\lambda \sim d^2$  (Fig. 4). In Supporting Information, we provide qualitative analytical explanations for these numerical results (Figs. S4 and S5). In particular, in section B of Supporting Information we derive an analytical approximation for the probability of chaos as a function of the dimension of phenotype space by arguing that a trajectory is chaotic if all fixed points of system (6) have at least one repelling direction, which becomes certain for large  $d$  due to the selective interactions between phenotypic components.

## Discussion

Ergodic chaos in long-term evolutionary dynamics offers two main conceptual perspectives. First, frequency-dependent ecological interactions can generate complicated evolutionary trajectories that visit all feasible regions of phenotype space in the long run even if the external environment (given by system parameters) is constant. In such situations, the current phenotypic state of a

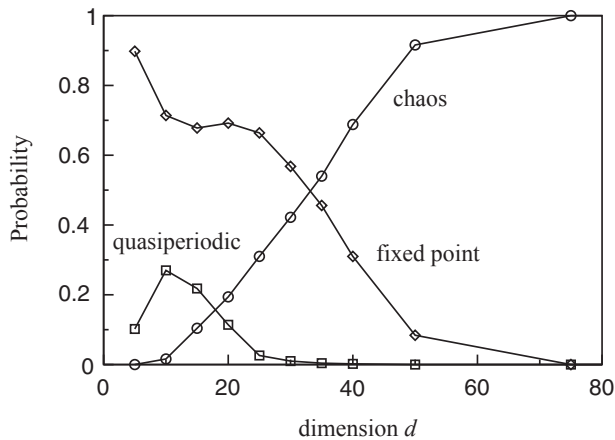


**Figure 2.** Percentage of different types of dynamics as a function of the dimensionality  $d$  of phenotype space. For each  $d$ , we generated 50 instances of the dynamical system (6) by choosing the coefficients  $b_{ij}$  and  $a_{ijk}$  randomly (see Fig. 1 legend) and then numerically integrating system (6) with 4 sets (single set for  $d = 200$ ) of random initial conditions. For each  $d$ , the figure shows the percentage of instances resulting in equilibrium dynamics with Lyapunov exponent  $\lambda < -0.1$  (squares), quasi-periodic dynamics with Lyapunov exponent  $-0.1 < \lambda < 0.1$  (diamonds), and chaos with Lyapunov exponent  $\lambda > 0.1$  (circles). Chaos starts to occur in a significant fraction of dynamical systems for  $d \approx 15$ , and starts to dominate for  $d \approx 35$ , with essentially no non-chaotic dynamics for  $d \geq 75$ .

population can never be understood as the result of an equilibrium or optimisation process, even though the process determining the phenotypic state is entirely adaptive and deterministic.

Second, chaotic evolutionary trajectories are intrinsically unpredictable. At the very basic level, biological evolution is stochastic, because the single-molecule events that correspond to spontaneous mutations are subject to fundamental, quantum mechanical randomness. The adaptive dynamics models considered here are defined on a coarse-grained time scale that is much larger than the typical time between mutations, and the models generate deterministic trajectories that are shaped by ecological interactions. However, mutations can in principle fundamentally alter chaotic long-term evolutionary trajectories due to sensitive dependence on initial conditions: whether a particular mutation occurs at a given point in time may slightly change the initial condition for the evolutionary trajectory unfolding after that time point, and this difference may translate into vastly different phenotypic states at much later points in time. It is important to note, however, that when the adaptive dynamics has a positive Lyapunov exponent and hence shows divergence along some composite direction in a high-dimensional phenotype space, divergence between trajectories in any given phenotypic component may take a long time (Fig. 5).

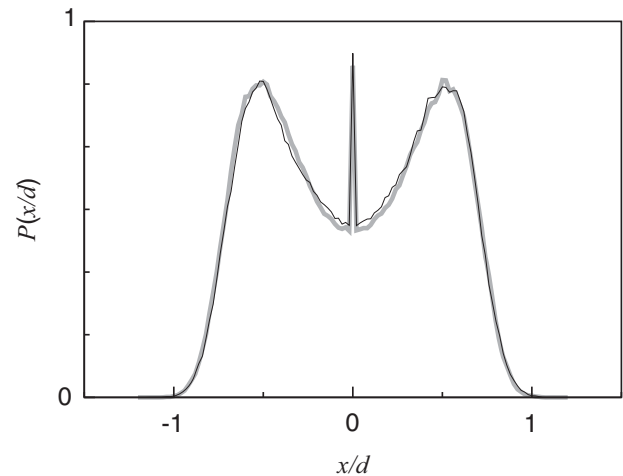


**Figure 3.** Examples of the density distributions  $P(x/d)$  for  $d = 100$  (thick grey line) and  $d = 150$  (thin black line) of the scaled state variable  $x/d$  (SI, section A) in an arbitrary component of phenotype space. Once the system is in the ergodic regime, the distribution is universal in the sense that it does not depend on the dimension  $d$  of phenotype space, on the particular choice of coefficients in (6), or on the phenotypic component. The distribution is obtained as a histogram over all the states that a system's trajectory attains during a long period of time. It shows two peaks lying symmetrically around the phenotype  $x = 0$ , which corresponds to the maximum of the carrying capacity function  $K(x)$ , and near which the system also spends part of its time, which is reflected in the third, central peak of the distribution  $P(x/d)$ .

This is because even if the largest Lyapunov exponent is positive, the total number of positive Lyapunov exponents usually represents a small fraction of the dimensionality of phenotype space. If we randomly choose a two-dimensional subspace of phenotype space, as for example in Figure 5, it is therefore likely that none of the coordinates in this subspace have a significant component in the directions with positive Lyapunov exponents. This explains the initial lack of divergence in the two projected trajectories shown in Figure 5. On the other hand, the probability that a projection of these two coordinates is exactly 0 in all directions with positive Lyapunov exponents is 0, and hence divergence will eventually occur if environmental conditions remain constant.

Nevertheless, even if evolutionary dynamics are chaotic, there may be many phenotypic components along which divergence would only occur over time scales at which the environment is likely to change as well, which would be reflected in change of the model parameters  $\beta_{ij}$  and  $\alpha_{ijk}$ . If this environmental change simplifies the evolutionary dynamics, then divergence would likely come to halt before it even started. However, if most combinations of model parameters result in chaos, which according to our results is likely with high-dimensional phenotypes, then environmental change would generate a different chaotic dynamics, and hence could result in divergence becoming stronger for

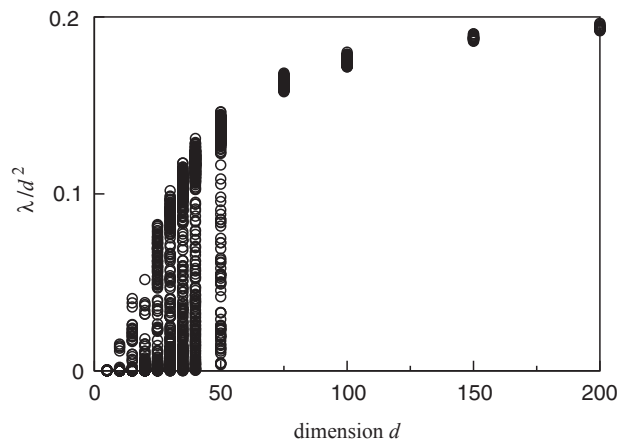


**Figure 4.** The scaled largest Lyapunov exponent  $\lambda/d^2$  (SI, section C) as a function of the dimension  $d$  of phenotype space, for the same data set as used for Figure 2. For large  $d$ , the largest scaled Lyapunov exponent saturates at an asymptotic value  $\lambda \approx 0.235 \cdot d^2$  (SI, section C).

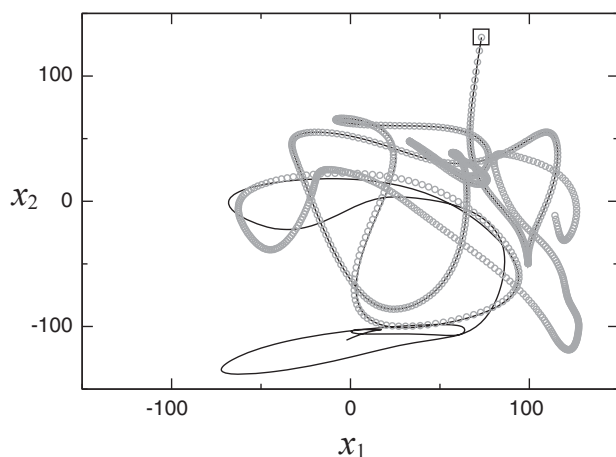


**Figure 5.** Example of divergence of two chaotic evolutionary trajectories (black line and grey circles) in  $d = 150$ -dimensional phenotype space. The trajectories start from initial conditions separated by a visually undetectable small distance  $\|\delta x_0\| = 10^{-3}$ . The initial positions of both trajectories are marked by a square at the top of the plot. The total time of evolution of both trajectories is  $100/d^2 \approx 0.0044$ . The spacing of the circles indicates the speed with which the trajectory unfolds. Divergence commences not immediately, but only after a noticeable transient period during which the two trajectories remain essentially indistinguishable.

certain phenotypes. Thus, evolutionary predictability of a particular phenotypic component hinges on the interactions between environmental change and chaotic dynamics. In any case, if the evolutionary dynamics are chaotic, then there is at least one (and usually several) direction in phenotype space in which trajectories are unpredictable over short time scales. In that sense, replaying

the tape of life (Gould 1989) could potentially result in completely different outcomes if evolution is chaotic.

These findings are, at least in principle, compatible with recent results obtained from long-term evolution experiments with *Escherichia coli* (Wiser et al. 2013), in which 12 replicate populations originating from a common ancestor have been evolving for more than 50,000 generations in a constant environment. Wiser et al. (2013) show that despite the simplicity and constancy of the environment, evolution has not yet come to halt, and instead growth rates of these bacteria have continually increased and are predicted to increase further without saturation. Moreover, substantial genetic and phenotypic differences have developed among all 12 populations, and the observed relative shortage of synonymous mutations reflects the adaptive rather than random nature of these differences. This indicates that evolution may indeed not be an equilibrium process in these experiments, and instead may exhibit complicated, unpredictable dynamics despite unfolding in a constant environment.

Our theoretical results are also relevant for the general problem of the prevalence of chaos in multidimensional dynamical systems. Chaos is well studied in high-dimensional Hamiltonian systems (Zaslavsky et al. 1991) (which are dynamical systems that are often used in physics and that are constrained by the requirement that volumes in phase space must be preserved by the dynamics), as well as in discrete-time systems of coupled oscillators with many degrees of freedom (Kaneko 1989; Ishihara and Kaneko 2005), but these results are not applicable to dissipative, non-Hamiltonian systems in continuous time, such as the adaptive dynamics models studied here. Surprisingly, our analysis may be the first systematic study of the occurrence of chaos in such systems as a function of the dimensionality of phase space.

Because the likelihood of chaotic evolutionary dynamics in our models is strongly influenced by the dimensionality of phenotype space, the biological relevance of our results hinges on the number of phenotypic properties affecting ecological interactions in real systems, and on the potential for selective interactions between these phenotypic properties. Given that metabolic networks of even the simplest bacterial organisms such as *E. coli* are incredibly complex (Selkov et al. 1996; Karp et al. 1999), it seems likely that in general, many phenotypic properties combine in complicated ways to affect ecological interactions such as competition for resources. Data testing this directly seems to be scant, but an indication for high dimensionality of ecologically relevant phenotype space comes, for example, from studies of the genetics of adaptive diversification in fishes (Keller et al. 2013) and in bacteria (Herron and Doebeli 2013). In pairs of fish species that have recently speciated into two different ecotypes, there is abundant genetic differentiation between the species, which is distributed over the whole genome. Some of this differentiation is due to differences in mating preferences, but it

appears that many of the observed genetic differences are related to ecological traits, and hence that many different genes affect ecological properties, and thus ecological interactions, of these fish (Keller et al. 2013). Similarly, a genetic analysis of adaptive diversification in evolution experiments with *E. coli* revealed that the diversified ecotypes that evolved from a single ancestral strain in about 1000 generations differed in many genes carrying adaptive mutations (Herron and Doebeli 2013). Other recent evolution experiments with *E. coli* showed the importance of epistasis, that is, nonadditive genetic effects, for evolutionary dynamics (Tenailon et al. 2012), which reflect selective interactions between different genotypes. Even if many genes are involved in responses to selection, it has been argued that the “effective dimensionality” of relevant genotype or phenotype space is low (e.g., Martin and Lenormand 2006; Kirkpatrick 2009), essentially because of genetic covariances between different traits, which can cause the covariance matrix to be singular, and hence some traits to be effectively linear combinations of other traits. However, even if the effective dimensionality is low and hence heritable variation is significant in only a few trait dimensions, there could still be some, albeit small variation in many other directions in phenotype space, which would warrant a high-dimensional analysis. For example, Tenailon et al. (2007) have argued that in viruses, phenotypic complexity, measured as the number of independent phenotypic components that affect fitness, tends to be quite high. It would seem to be an important empirical endeavor to gain a general understanding of the number of independent phenotypic properties that can be expected to affect ecological interactions, and of the degree of selective interactions between them.

Even if one accepts the premise of high-dimensional phenotype spaces, one could question the realism of the logistic competition models used here. Although it is true that our models do not derive from an underlying mechanistic model for ecological interactions between individual organisms, we point out that logistic competition models have been used very widely in both ecological and evolutionary theory. Moreover, our approach examines in some sense all possible models for the evolutionary dynamics of  $d$  phenotypes whose trajectories are confined to a bounded region in phenotype space, regardless of the ecological interactions that generate the evolutionary dynamics of those phenotypes. This is because the coefficients  $b_{ij}$  and  $\alpha_{ijk}$  in (6) are arbitrary, and hence to second order, any such model will have the general form (6). In that sense, the model (6) is general, even though it was derived from a particular competition model. In particular, the subset of “realistic” models, that is, the subset of those models that can be derived mechanistically from underlying ecological interactions, will have this form. Thus, if essentially all models of the form (6) have chaotic dynamics for high  $d$ , then any particular “realistic” model is likely to have such dynamics as well.

Our results rely on the use of adaptive dynamics for modeling evolutionary dynamics, and their generality therefore also hinges on the assumptions underlying the adaptive dynamics approach, which have been discussed in detail elsewhere (e.g., Waxman and Gavrillets 2005, as well as responses in the same journal issue). Essentially, adaptive dynamics describes the evolutionary dynamics of phenotype distributions that are given as Dirac  $\delta$ -function, and hence have infinitely small variance (i.e., there is no standing genetic variation, and mutations are assumed to be rare and to have small effects). An equivalent formalism would result with the traditional quantitative genetics approach (e.g., Lande 1979) under the commonly made assumption that phenotype distributions are multivariate Gaussian with fixed variances. For logistic competition of the type considered here, this would result in a system of differential equations of the form (6), in which the variables would be the means of the various phenotypic components. Considering the dynamics of more general and more flexible phenotype distributions is an interesting problem, but it would require different formalisms, for example, high-dimensional partial differential equations or individual-based models. Using such formalisms would, for example, also allow for an investigation of evolutionary diversification (i.e., the emergence of multimodal phenotype distributions) along complicated, high-dimensional evolutionary trajectories. However, such questions are beyond the scope of this work.

For now, our results warrant at least a critical re-examination of the generality of simple equilibrium and optimization dynamics in evolution. Forty years ago, the realization that simple ecological models can have very complicated dynamics revolutionized ecological thinking (May 1976). Our high-dimensional models are not simple, but they show that nonlinear evolutionary feedbacks generated by frequency-dependent ecological interactions can also lead to very complicated dynamics. In fact, with frequency dependence most evolutionary dynamics may be chaotic when phenotypes are high-dimensional. In general, evolution is a complicated dynamical system driven by birth and death events that are determined by many different factors, such as external biotic and abiotic conditions, current phenotype distributions, age and physiological condition, etc. If birth and death rates are complicated functions of many different factors that change themselves as evolution unfolds, we do not see any reason to expect that in general, evolutionary dynamics should be simple (after all, it is, e.g., well known that weather often exhibits chaos and long-term unpredictability, essentially because of the nonlinearity of the dynamics and the complexity of the interactions among the many different components determining the weather). Nevertheless, our perception is that to date, evolutionary biologists are unaware of the fact that general evolutionary dynamics in continuous phenotype spaces of high dimensions are likely to

be complicated (but see (Wiser et al. 2013)). Knowing that, in principle, long-term evolutionary complexity can be due to intrinsic frequency-dependent interactions rather than simply to changes in the external environment would generally seem to be useful, in the same way as it was useful when, four decades ago, ecologists became aware of the possibility of chaos due to nonlinear interactions in generic ecological models.

## ACKNOWLEDGMENTS

It was supported by FONDECYT (Chile) project 1110288. MD was supported by NSERC (Canada).

## LITERATURE CITED

- Altenberg, L. 1991. Chaos from linear frequency-dependent selection. *Am. Nat.* 138:51–68.
- Bak, P., C. Tang, and K. Wiesenfeld. 1987. Self-organized criticality: an explanation of the  $1/f$  noise. *Phys. Rev. Lett.* 59:381–384.
- Dercole, F., and S. Rinaldi. 2008. Analysis of evolutionary processes: the adaptive dynamics approach and its applications. Princeton Univ. Press, Princeton, NJ.
- Dercole, F., R. Ferrière, A. Gragnani, and S. Rinaldi. 2006. Coevolution of slow-fast populations: evolutionary sliding, evolutionary pseudo-equilibria and complex red queen dynamics. *Proc. Roy. Soc. B* 273:983–990.
- Devaney, R. L. 1986. Introduction to chaotic dynamical systems. Benjamin/Cummings, Menlo Park, CA.
- Dieckmann, U., and R. Law. 1996. The dynamical theory of coevolution: a derivation from stochastic ecological processes. *J. Math. Biol.* 34:579–612.
- Dieckmann, U., P. Marrow, and R. Law. 1995. Evolutionary cycling in predator-prey interactions: population-dynamics and the red queen. *J. Theor. Biol.* 176:91–102.
- Doebeli, M. 2011. Adaptive diversification. Princeton Univ. Press, Princeton, NJ.
- Doebeli, M., and U. Dieckmann. 2000. Evolutionary branching and sympatric speciation caused by different types of ecological interactions. *Am. Nat.* 156:S77–S101.
- Doebeli, M., and Y. Ispolatov. 2010. Complexity and diversity. *Science* 328:493–497.
- Edelman, A. 1997. The probability that a random real gaussian matrix has  $k$  real eigenvalues, related distributions, and the circular law. *J. Multivar. Anal.* 60:203–232.
- Gavrilets, S. 2004. Fitness landscapes and the origin of species. Princeton Univ. Press, Princeton, NJ.
- Gavrilets, S., and A. Hastings. 1995. Intermittency and transient chaos from simple frequency-dependent selection. *Proc. Roy. Soc. Lond. B* 261:233–238.
- Geritz, S. A. H., E. Kisdi, G. Meszéna, and J. A. J. Metz. 1998. Evolutionarily singular strategies and the adaptive growth and branching of the evolutionary tree. *Evol. Ecol.* 12:35–57.
- Gilman, R. T., S. L. Nuismer, and D.-C. Jhwueng. 2012. Coevolution in multidimensional trait space favours escape from parasites and pathogens. *Nature* 483:328–330.
- Gleick, J. 1988. Chaos: making a new science. Penguin, New York.
- Gould, S. J. 1989. Wonderful life: the burgess shale and the nature of history. Norton, New York.
- Heino, M., J. Metz, and V. Kaitala. 1998. The enigma of frequency-dependent selection. *Trends Ecol. Evol.* 13:367–370.
- Herron, M. D., and M. Doebeli. 2013. Parallel evolutionary dynamics of adaptive diversification in *E. coli*. *PLOS Biol.* 11:e1001490.
- Ishihara, S., and K. Kaneko. 2005. Magic number  $7 \pm 2$  in networks of threshold dynamics. *Phys. Rev. Lett.* 94:058102.
- Kaneko, K. 1989. Pattern dynamics in spatiotemporal chaos. *Physica D* 34:1–41.
- Karp, P., M. Riley, S. Paley, A. Pellegrini-Toole, and M. Krummenacker. 1999. Eco Cyc: encyclopedia of *Escherichia coli* genes and metabolism. *Nucleic Acids Res.* 27:55–58.
- Keller, I., C. E. Wagner, L. Greuter, S. Mwaiko, O. Selz, A. Sivasundar, S. Wittwer, and O. Seehausen. 2013. Population genomic signatures of divergent adaptation, gene flow and hybrid speciation in the rapid radiation of lake victoria cichlid fishes. *Mol. Ecol.* 22:2848–2863.
- Kirkpatrick, M. 2009. Patterns of quantitative genetic variation in multiple dimensions. *Genetica* 136:271–284.
- Lande, R. 1979. Quantitative genetic-analysis of multivariate evolution, applied to brain-body size allometry. *Evolution* 33:402–416.
- Leimar, O. 2009. Multidimensional convergence stability. *Evol. Ecol. Res.* 11:191–208.
- Li, T., and J. Yorke. 1975. Period three implies chaos. *Am. Math. Mon.* 82:985–992.
- Martin, G., and T. Lenormand. 2006. A general multivariate extension of Fisher's geometrical model and the distribution of mutation fitness effects across species. *Evolution* 60:893–907.
- May, R. M. 1976. Simple mathematical models with very complicated dynamics. *Nature* 261:459–467.
- Nowak, M. A., and K. Sigmund. 1993. Chaos and the evolution of cooperation. *Proc. Nat. Acad. Sci. USA* 90:5091–5094.
- Priklopil, T. 2012. Chaotic dynamics of allele frequencies in condition-dependent mating systems. *Theor. Popul. Biol.* 82:109–116.
- Schluter, D. 2000. The ecology of adaptive radiation. Oxford Univ. Press, Oxford, U.K.
- Schneider, K. A. 2008. Maximization principles for frequency-dependent selection I: the one-locus two-allele case. *Theor. Popul. Biol.* 74:251–262.
- Selkov, E., S. Basmanova, T. Gaasterland, I. Goryanin, Y. Gretchkin, N. Maltsev, V. Nenashev, R. Overbeek, E. Panyushkina, L. Pronevitch, et al. 1996. The metabolic pathway collection from EMP: the enzymes and metabolic pathways database. *Nucleic Acids Res.* 24:26–28.
- Svensson, E. I., and R. Calsbeek (eds.). 2012. The adaptive landscape in evolutionary biology. Oxford Univ. Press, Oxford, U.K.
- Tenaillon, O., O. K. Silander, J. P. Uzan, and L. Chao. 2007. Quantifying organismal complexity using a population genetic approach. *PLOS One* 2:e217. doi:10.1371/journal.pone.0000217.
- Tenaillon, O., A. Rodríguez-Verdugo, R. L. Gaut, P. McDonald, A. F. Bennett, A. D. Long, and B. S. Gaut. 2012. The molecular diversity of adaptive convergence. *Science* 335:457–461.
- Waxman, D., and S. Gavrilets. 2005. 20 questions on adaptive dynamics. *J. Evol. Biol.* 918:1139–1154.
- Wiser, M. J., N. Ribeck, and R. E. Lenski. 2013. Long-term dynamics of adaptation in asexual populations. *Science* 342:1364–1367.
- Wright, S. 1932. The roles of mutation, inbreeding, crossbreeding, and selection in evolution. Pp. 355–366 in Proceedings of the 6th international congress on genetics. Brooklyn Botanic Gardens, Menasha, WI.
- Zaslavsky, G. M., R. Z. Sagdeev, D. A. Usikov, and A. A. Chemikov. 1991. Weak chaos and quasi-regular patterns. Cambridge Univ. Press, Cambridge, U.K.

Associate Editor: A. Agrawal

## Appendix

Here we describe how the largest Lyapunov exponent is calculated. For each trajectory obtained through numerical integration of the adaptive dynamics (6), the time average of the largest Lyapunov exponent  $\lambda$  was calculated as follows. Every  $\tau$  time units the trajectory was slightly perturbed,  $x' = x + \delta x_0$ , by a vector with a constant magnitude  $\|\delta x_0\|$  and a random direction. Both resulting trajectories were propagated for  $\tau$  time units, after which the distance between the perturbed and unperturbed positions  $\|\delta x_\tau\|$  was recorded. The largest Lyapunov exponent was calculated for each  $\tau$  time units as

$$\lambda = \frac{1}{\tau} \ln \left( \frac{\|\delta x_\tau\|}{\|\delta x_0\|} \right), \quad (\text{A.1})$$

and subsequently averaged over the trajectory. Visual inspection of sample trajectories led us to designate the following categories: Trajectories with  $\lambda > 0.1$  are called chaotic, trajectories

with  $|\lambda| < 0.1$  are called quasi-periodic, and trajectories with  $\lambda < -0.1$  are called fixed points.

Choosing suitable time intervals  $\tau$  for the numerical calculations of the largest Lyapunov exponent is constrained on both sides. On the one hand, values of  $\tau$  that are too small do not leave sufficient time for a randomly chosen direction of perturbation to align itself with the direction of the fastest divergence corresponding to the largest Lyapunov exponent. On the other hand, for values of  $\tau$  that are too large the divergent trajectories reach the limit of the available phenotype space and fold back, so that the distance between them saturates. Both scenarios result in the underestimation of the distance between trajectories and the resulting value of the largest Lyapunov exponent. Thus the optimal value of  $\tau$  is the one giving the maximum average value of the largest Lyapunov exponent. Our numerical experiments indicate that the optimal values of  $\tau$  lie in the range between  $10^{-5}$  and  $10^{-3}$ , with the smaller values better suited for higher dimensions  $d$ .

### Supporting Information

Additional Supporting Information may be found in the online version of this article at the publisher's website:

**Figure S1.** Scaling of the mean square of a coordinate  $x_i$  with the dimensionality of phenotype space,  $\sqrt{\langle x_i^2 \rangle} \sim d$ .

**Figure S2.** Examples of projections of ergodic chaotic trajectories for  $d = 15$  (magenta),  $d = 30$  (blue),  $d = 50$  (dark blue),  $d = 75$  (yellow),  $d = 100$  (green),  $d = 150$  (red), and  $d = 200$  (black).

**Figure S3.** Examples of projections of ergodic chaotic trajectories system (6) (main text) when the coefficients  $b_{ij}$  and  $a_{ijk}$  were divided by  $\sqrt{d}$  and  $d$ , respectively;  $d = 75$  (red), and  $d = 100$  (black).

**Figure S4.** The numerically measured probability of occurrence of chaos (black line; data from Fig. 2 in the main text) and the estimate (S5) with  $P_n = 0.85$  (red line), which shows a reasonable fit.

**Figure S5.** The slow convergence to the asymptotic regime of the average largest Lyapunov exponent  $\lambda$  (black circles; same as Fig. 4 in main text) is explained using the extreme value statistics given by equation (S12) (red line).